PHYSICAL REVIEW B **66**, 140514(R) (2002)

^{11}B and ^{27}Al NMR spin-lattice relaxation and Knight shift of $Mg_{1-x}Al_xB_2$: Evidence for an anisotropic Fermi surface

G. Papavassiliou,[1] M. Pissas,[1] M. Karayanni,[1] M. Fardis,[1] S. Koutandos,[1] and K. Prassides[1,2]
[1]*Institute of Materials Science, NCSR, Demokritos, 153 10 Aghia Paraskevi, Athens, Greece*
[2]*School of Chemistry, Physics and Environmental Science, University of Sussex, Brighton BN1 9QJ, United Kingdom*
(Received 23 September 2002; published 31 October 2002)

We report a detailed study of the ^{11}B and ^{27}Al NMR spin-lattice relaxation rates ($1/T_1$) and the ^{27}Al Knight shift (K) in $Mg_{1-x}Al_xB_2$, $0 \leqslant x \leqslant 1$. The evolution of $(1/T_1T)$ and K with x is in excellent agreement with the prediction of *ab initio* calculations of a highly anisotropic Fermi surface, consisting mainly of hole-type two-dimensional (2D) cylindrical sheets from bonding $2p_{x,y}$ boron orbitals. The density of states at the Fermi level also decreases sharply on Al doping and the 2D sheets collapse at $x \approx 0.55$, where the superconducting phase disappears.

DOI: 10.1103/PhysRevB.66.140514 PACS number(s): 74.25.−q, 74.70.Dd, 76.60.Es

Superconductivity in MgB_2 has recently received much interest,[1] as this binary alloy displays a remarkably high T_c of ≈ 40 K. MgB_2 is isostructural and isoelectronic with intercalated graphite (ICG), with carbon replaced by boron, and therefore exhibits similar bonding and electronic properties as ICG. Thus the high T_c value of MgB_2 in comparison with ICG (~ 5 K) was very surprising. Band structure calculations[2–6] have shown that Mg is substantially ionized in this compound. However, the electrons donated to the system are not localized on the B anions, but are rather distributed over the whole crystal. The six B p bands contribute mainly at the Fermi level. The unique feature of MgB_2 is the incomplete filling of the two σ bands corresponding to predominantly covalent sp^2-hybridized bonding within the graphite-like boron layers. Two isotropic π bands are derived from B p_z and four two-dimensional (2D) σ bands from B $p_{x,y}$ states. Both p_z bands cross the Fermi level, while only two bonding $p_{x,y}$ bands and only near the Γ point (0,0,0) do so, forming cylindrical Fermi surfaces around the Γ-A line. Due to their 2D character, the latter contribute more than 30% of the total density of states (DOS).[2,4,7,8] The strong anisotropy in the Fermi surface (and possibly in the electron phonon coupling) agrees with the reported anisotropy in H_{c2},[9–14] and the existence of two superconducting gaps.[15–21]

In view of these findings, there is considerable interest in the properties of electron- or hole-doped MgB_2, in order to follow the dependence of the electron DOS and the Fermi surface on doping. A suitable substituent for such a study is Al, which donates three electrons (instead of two for Mg), and thus leads to doping by one electron per Mg atom. In addition, the MgB_2 and AlB_2 end members and the intermediate phases, $Mg_{1-x}Al_xB_2$ crystallize in the same $P6/mmm$ space group and increasing Al doping leads to an almost linear decrease of the boron interlayer spacing.[22] The similarity of the calculated electronic density of states between MgB_2 and AlB_2 indicates that Al doping results in simple filling of the available electronic states. Suzuki *et al.*[23] predicted that the concentration of σ holes in $Mg_{1-x}Al_xB_2$ varies with x as $n_h = (0.8 - 1.4x) \times 10^{22}$ cm^{-3}, leading to $n_h = 0$ for $x \approx 0.6$. A similar conclusion was reached in Refs. 3,4,24. The detrimental effect of Al doping on T_c can then be explained by the increase in the Fermi energy (E_F) and the decrease of $N(E_F)$ with increasing doping level x. An excellent probe to study the influence of Al substitution on the electronic structure of electron doped MgB_2 is nuclear magnetic resonance (NMR). Knight shift, K, and nuclear spin-lattice relaxation (NSLR) rate, $1/T_1$, measurements can lead to the experimental determination of $N(E_F)$ through the static and fluctuating parts of the hyperfine field, induced at the position of the resonating nuclei by the electrons at the Fermi surface. The contribution of different atoms to $N(E_F)$ and the anisotropy of the electronic states at the Fermi level can then be estimated. The Hamiltonian describing the magnetic interaction of the nucleus with the atomic electrons can be written as,[25] $\mathcal{H} = 2(8\pi/3)\mu_B\gamma_n\hbar\mathbf{I}\cdot\mathbf{S}(\mathbf{r})\delta(\mathbf{r}) - 2\mu_B\gamma_n\hbar\mathbf{I}\cdot[\mathbf{S}/r^3 - 3\mathbf{r}(\mathbf{S}\cdot\mathbf{r})/r^5] - \gamma_n\hbar(e/mc)[\mathbf{I}\cdot(\mathbf{r}\times\mathbf{p})/r^3]$, where μ_B is the Bohr magneton, γ_n the gyromagnetic ratio, $\mathbf{I}$ and $\mathbf{S}$ the nuclear and electron spins, and $\mathbf{r}$ is the radius vector of the electron with the nucleus at the origin. The first term in the above equation describes the Fermi-contact interaction, the second term the spin dipolar interaction between nuclear and electron spins, and the third term the coupling with the electronic orbital moment. In the simplest case, where only contribution from the Fermi contact term is considered, the first term can be rewritten as $\mathcal{H}_{KS} \propto -V(8\pi/3)\gamma_n\hbar\chi_p\langle|\Psi(0)|^2\rangle_{F_S}\mathbf{I}\cdot\mathbf{H}_0$, where $\chi_p = M/H = \mu_B^2 N_s(E_F)/V$, and the symbol $\langle\rangle_{F_S}$ denotes the average over all s orbitals at the Fermi surface. Due to this term, the nuclear spin $\mathbf{I}$ "sees" an internal field $V\chi_p\mathbf{H}_0/2\mu_B$, which is superimposed on the applied external magnetic field and causes a paramagnetic shift of the nuclear resonance, i.e., the Knight shift. In a similar way, the relaxation rate from the Fermi-contact term is expressed as[25] $(1/T_1) = (64\pi^3/9)\gamma_e^2\gamma_n^2\hbar^3\langle|\Psi_{\mathbf{k}}(0)|^2|\Psi_{\mathbf{k}'}(0)|^2\rangle_F N_s(E_F)^2 k_B T$. A similar dependence on $N_{2p}(E_F)^2$ is found when the nuclear Hamiltonian is dominated by the nuclear-electron orbital interaction.[26] Hence, the dependence of both K and $1/T_1$ on the partial $N_i(E_F)$ can be derived.

Until now ^{11}B, ^{27}Al, and ^{25}Mg NSLR and Knight shift measurements have been reported for pure MgB_2 and AlB_2.[27–31] These results, in conjunction with *ab initio*

calculations[4,7,8] have shown that the ^{11}B NSLR is dominated by orbital relaxation in MgB_2 and by the Fermi-contact interaction in AlB_2. On the other hand, the ^{27}Al and ^{25}Mg NSLR rates and the Knight shift on all three (^{11}B, ^{27}Al, and ^{25}Mg) sites were shown to be controlled by the Fermi-contact polarization.[7,29] In addition, ^{11}B-NMR NSLR relaxation rate measurements on mixed $Mg_{1-x}Al_xB_2$, $x \leqslant 0.2$, have revealed a rapid decrease of $1/(T_1T)$ with doping that was attributed to the reduction of the total $N(E_F)$.[32] However, a detailed NMR study of the variation of each partial $N_i(E_F)$ with Al doping and comparison with theory is so far lacking.

The purpose of this work is to report a systematic study of the ^{11}B and ^{27}Al NSLR rates, $1/T_1$ and the ^{27}Al Knight shifts as a function of Al doping for $Mg_{1-x}Al_xB_2$, $0 \leqslant x \leqslant 1$. ^{11}B Knight shift measurements were not considered because the isotropic ^{11}B Knight shift is small [$+40$ ppm for MgB_2 and -10 ppm for AlB_2 (Ref. 29)] and of the same order of magnitude as the dipolar and the second order quadrupolar split at the fields of 2.35 and 4.7 T used in this work. Our measurements show explicitly (i) the validity of theoretical calculations based on local density-functional methods[4,8] of the boron $^{11}(1/T_1T)$ evolution with Al doping and (ii) the dominance of the orbital relaxation up to $x \approx 0.55$, where $T_c(x)$ vanishes. This is convincing evidence that up to $x \approx 0.55$, the hole-type 2D cylindrical sheets (from bonding $2p_{x,y}$ boron orbitals) of the Fermi surface play an essential role in the ^{11}B NSLR. The slight decrease of both ^{27}K and $^{27}(1/T_1T)$ as x increases from 0 to 0.55 and the subsequent abrupt increase for $x \geqslant 0.55$ also support this conclusion.

Polycrystalline samples of nominal composition $Mg_{1-x}Al_xB_2$ ($0 \leqslant x \leqslant 1$) were prepared by reaction of Al and Mg powders with amorphous B at temperatures between 700°C and 910°C as described elsewhere.[14] We find that (i) the temperature where the reaction (preparation temperature) takes place sensitively affects the appearance of the $(00l)$ diffraction peaks for $0.05 \leqslant x \leqslant 0.5$ (Refs. 22,33–35)—significant broadening and/or splitting of these reflections are signatures of multiphase behavior in this doping range and (ii) carefully prepared samples in the region arround $x = 0.5$ show the presence of a broad superlattice peak, $(0\,0\,\frac{1}{2})$ arising from ordering of Mg and Al layers.[36] ^{27}Al NMR line shape measurements of the central transition $(-1/2 \rightarrow 1/2)$ were performed on two spectrometers operating at external magnetic fields $H_0 = 2.35$ and 4.7 T. Spectra were obtained from the Fourier transform of half of the echo, following a typical $\pi/2 - \tau - \pi/2$ solid spin-echo pulse sequence. The spectra for the $x = 0.0125$ and 0.025 Al doping concentrations were extremely weak and therefore 100 000 signal accumulations were needed for a satisfactory signal-to-noise ratio. The ^{11}B T_1 of the central line was determined by applying a single pulse saturation recovery technique, and recording the growth of the solid echo at variable delay times. The T_1 values were obtained by fitting the relaxation function, $m(t) = (M(\infty) - M(t))/M(\infty) = 0.1\exp(-t/T_1) + 0.9\exp(-6t/T_1)$.[37] Correspondingly, ^{27}Al T_1 was determined by applying the three-exponential recovery law that is appropriate for $I = 5/2$ nuclei.[30,37]

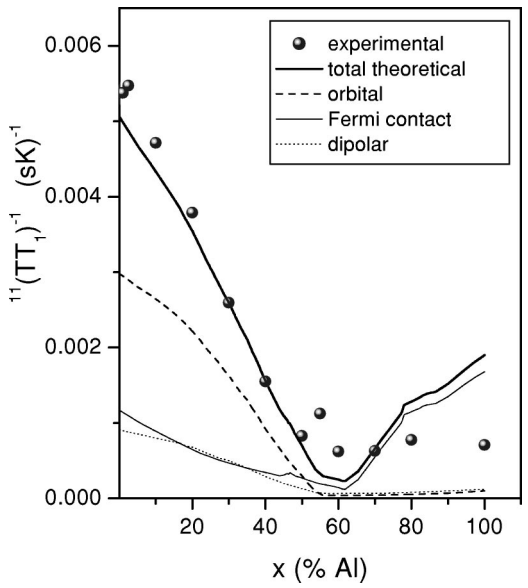

FIG. 1. Boron $^{11}(1/T_1T)$ for $Mg_{1-x}Al_xB_2$ as a function of Al doping. The lines show the results of the *ab initio* calculations of Refs. 4, 8.

Figure 1 shows the boron $^{11}(1/TT_1)$ as a function of x in the normal state. In all cases the magnetization recovery curves were nicely fitted with a single T_1 component. In addition, a $1/T_1T =$ constant relation was found to fit the experimental data in the whole normal state, for all doping concentrations. The $^{11}(1/TT_1)$ values in Fig. 1 are the results of the fits in the temperature range 300–80 K. Our measurements reveal that as the doping increases, $^{11}(1/TT_1)$ decreases rapidly up to $x = 0.55$, and then shows a slight increase for $x \geqslant 0.55$. For reasons of comparison, we have also included the calculated $^{11}(1/TT_1)$ values from Ref. 8 for all three orbital, dipole-dipole, and Fermi-contact term contributions. Clearly, the orbital term dominates in the ^{11}B relaxation rates for $x \leqslant 0.55$. In the case of pure MgB_2, the ^{11}B orbital hyperfine interaction of $2p$ holes with the nuclear magnetic moments is about three times larger than the dipole-dipole and the Fermi-contact interaction. This is due to the fact that the boron p_σ and p_π bands are all at the Fermi level ($N_{px} = N_{py} \approx 0.035$, $N_{pz} \approx 0.045$ states/eV/spin/B), whereas only a few s boron electrons are close to the Fermi level ($N_s \approx 0.002$ states/eV/B).[7,29] This gives a ratio between the Fermi-contact and the orbital/dipole-dipole coupling constants, $F \simeq 0.35$,[7] and $^{11}(1/TT_1)$ is mainly proportional to $N_{2p}(E_F)^2$. By Al, i.e., electron doping, $^{11}(1/TT_1)$ decreases rapidly, while for $x \geqslant 0.6$ it gives a p-state anisotropy ratio $N_{px}/N_{pz} \approx 0.1$, as predicted for AlB_2.[8] It may thus be inferred that the rapid decrease of the ^{11}B relaxation rate is due to the decrease of the DOS in the 2D hole-type sheets. A minimum $^{11}(1/TT_1)$ value is obtained at $0.55 \leqslant x \leqslant 0.60$, where the 2D sheets appear to collapse. We also note a discrepancy between the theoretical and experimental values for $x > 0.6$. Most probably, calculations tend to overestimate the

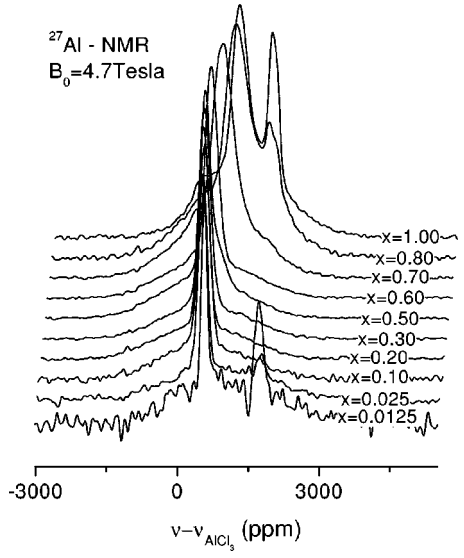

FIG. 2. ^{27}Al NMR line shapes of the central transition at room temperature for $Mg_{1-x}Al_xB_2$. For clarity, all spectra are normalized to 1. In this scaling, spectra for $x=0.0125$ and 0.025 are multiplied by a factor of 100 and 50, respectively, in comparison to the spectrum of AlB_2.

Fermi-contact interaction at the position of the B nucleus in this doping range.[29]

Figure 2 shows the ^{27}Al NMR line shapes for $Mg_{1-x}Al_xB_2$ at room temperature in a field of 4.7 T. A completely similar picture was obtained at 2.35 T. In the doping region $0.1 \leqslant x \leqslant 0.7$, the spectra consist of a single central transition line, which shifts in frequency with doping, and a broad powder pattern from the satellite transitions. As x increases, line broadening is observed, reaching $\approx$20 kHz for AlB_2. This may be attributed to increasing Al-B dipolar broadening, probably due to the strong decrease of the interlayer distance with Al doping. For $x=$ 0.80 and 1.0, a second signal is observed at $+1700$ ppm, arising from unreacted Al which is present at high doping concentrations. The assignment of this peak was confirmed following comparisons with the ^{27}Al NMR signal from powder Al. In addition, a weak spurious peak, arising from the probe was also observed at $+1700$ ppm for $x=0.0125$ and 0.025. We note that all line shapes could be well fitted with single Gaussians and no signatures of the phase separation, reported by x-ray diffraction[22,33–36] were observed in the ^{27}Al (and ^{11}B) spectra for $0.05 \leqslant x \leqslant 0.50$. This might imply that NMR, which is sensitive in the MHz spectral region, probes only the average electronic structure of multiphase samples.

In Fig. 3 we show the shift of the central line peak as a function of x, in fields 2.35 and 4.7 T. The signal of a standard aqueous solution of $AlCl_3$ was used as reference. The coincidence of the curves in both fields is a clear evidence that the obtained spectral shift corresponds solely to the ^{27}K shift. In typical shifts of $I=5/2$ nuclei like ^{27}Al from the reference sample, in addition to the Knight shift the center-of-gravity position of the NMR signal should include the second-order quadrupole shift given by $\Delta\nu = (25\nu_Q^2)/(18\nu_L)$.[38] However, recent experiments on AlB_2

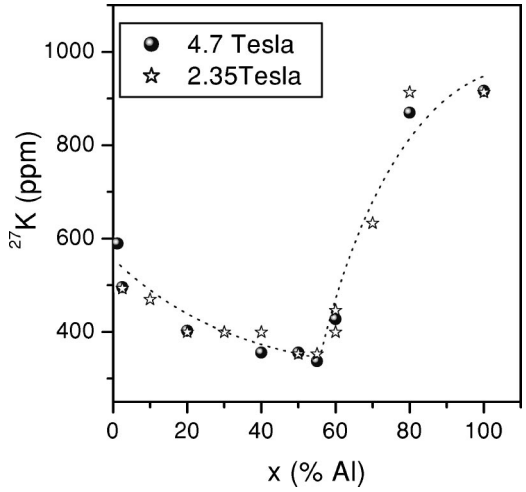

FIG. 3. The ^{27}K Knight shift of NMR spectra for $Mg_{1-x}Al_xB_2$ in fields 2.35 and 4.7 T.

have shown that the quadrupolar coupling constant is $\nu_Q \simeq 80$ kHz,[29] thus giving a second order quadrupolar shift, which in case of the fields used in this work, is as small as a fraction of 1 kHz. According to Fig. 3, by increasing x the ^{27}K decreases rapidly, whereas for $x \geqslant 0.55$, i.e., at the doping value where the superconductive phase disappears,[24] it increases sharply becoming $\approx +900$ ppm for pure AlB_2. As previously shown, by Al doping of MgB_2 the σ hole bands are filled,[3,4,24] and their contribution to $N(E_F)$ becomes zero at $x \approx 0.55$[24]. Evidently, the gradual decrease of ^{27}K for $x \leqslant 0.55$ reflects (i) the initial slight decrease of $N_s(E_F)$ in this doping range,[2] and (ii) the reduction of the Stoner enhancement by filling the σ hole bands, due to decrease of the total $N(E_F)$. We notice that the Stoner enhancement renormalizes both K and $1/T_1$ by a factor $S_o = 1/(1-IN(E_F))^{\alpha}$, with $\alpha = 1$ for K, and $1 \leqslant \alpha \leqslant 2$ for $1/T_1$.[7,8] On the other hand, the sharp increase of the Knight shift for $x \geqslant 0.55$, may be attributed to the rapid increase of N_s by further doping, after completely filling the $2p_{x,y}$ hole bands [N_s(Mg) in MgB_2 is ≈ 0.0092 states/eV/spin, whereas N_s(Al) in AlB_2 is

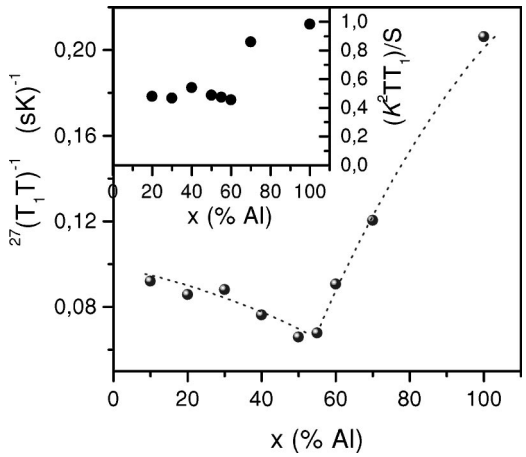

FIG. 4. $^{27}(1/T_1T)$ for $Mg_{1-x}Al_xB_2$ as a function of Al-doping x. The inset demonstrates the Korringa ratio R, as a function of x.

≈ 0.0362 states/eV/spin.[7]] A similar behavior is observed in Fig. 4, which exhibits the $^{27}(1/TT_1)$ vs x plot. In the inset weshow the Korringa ratio,[39] $R=(K^2T_1T)/S$, where $S=(\gamma_e/\gamma_n)^2\cdot(\hbar/2)^2k_B=0.387\times10^{-5}$ s K for ^{27}Al. Here, γ_e, γ_n are the gyromagnetic ratios for the electron and nucleus, respectively. It is observed that while $R\approx1$ for pure AlB_2, i.e., the ideal value of unity for s electrons, it goes to $\simeq0.5$ for $x\leqslant0.6$. This implies that for pure AlB_2 the Fermi-contact interaction is the dominant mechanism responsible for relaxation and Knight shift at the Al site. However, for $x\leqslant0.6$ there is a considerable orbital contribution in the relaxation rate. Apparently by Al doping, a part of the donated electrons that is transferred to the π bonds,[24] gives rise to an increase of the orbital contribution to the relaxation.

In conclusion, ^{11}B and ^{27}Al NMR NSLR rate in the temperature range 300 K–80 K, and Knight shift measurements at room temperature, have been employed in order to investigate the structure and the variation of the Fermi surface in MgB_2 upon Al (i.e., electron) doping. Our results are completely consistent with calculations predicting a strongly anisotropic Fermi surface that is comprised from hole-type σ-bonding 2D cylindrical sheets, and a hole-type and electron-type, 3D π-bonding tubular network. The collapse of the 2D sheets at $x\simeq0.55$, as predicted by theory, is experimentally verified by the fast decrease of the ^{11}B NSLR rate for $x\leqslant0.55$ and the sharp increase of both the ^{27}K and ^{27}NSLR rates for $x\geqslant0.55$. The latter indicates a strong reshaping of the Fermi surface towards the electronic structure of AlB_2, due to interplane electron contribution. Our results concile with both experimental and theoretical evidence that indicate anisotropic pairing and multigap superconductivity in MgB_2.

[1] J. Nagamatsu *et al.*, Nature (London) **410**, 63 (2001).
[2] J. Kortus *et al.*, Phys. Rev. Lett. **86**, 4656 (2001).
[3] J.M. An and W.E. Pickett, Phys. Rev. Lett. **86**, 4366 (2001).
[4] K.D. Belashchenko *et al.*, Phys. Rev. B **64**, 092503 (2001); V.P. Antropov *et al.*, cond-mat/0107123 (unpublished).
[5] Y. Kong *et al.*, Phys. Rev. B **64**, 020501(R) (2001).
[6] P.P. Singh, Phys. Rev. Lett. **87**, 087004 (2001).
[7] E. Pavarini *et al.*, Phys. Rev. B **64**, 140504 (2002).
[8] K.D. Belashchenko *et al.*, Phys. Rev. B **64**, 132506 (2001).
[9] O.F. de Lima *et al.*, Phys. Rev. Lett. **86**, 5974 (2001).
[10] S. Patnaik *et al.*, Semicond. Sci. Technol. **14**, 315 (2001).
[11] F. Simon *et al.*, Phys. Rev. Lett. **87**, 047002 (2001).
[12] S.L. Bud'ko *et al.*, Phys. Rev. B **64**, 180506 (2001).
[13] G. Papavassiliou *et al.*, Phys. Rev. B **65**, 012510 (2002).
[14] M. Pissas *et al.*, Phys. Rev. B **65**, 184514 (2002).
[15] F. Bouquet *et al.*, Phys. Rev. Lett. **87**, 047001 (2001).
[16] Amy Y. Liu *et al.*, Phys. Rev. Lett. **87**, 087005 (2001).
[17] P. Szabo *et al.*, Phys. Rev. Lett. **87**, 137005 (2001).
[18] X.K. Chen *et al.*, Phys. Rev. Lett. **87**, 157002 (2001).
[19] S. Tsuda *et al.*, Phys. Rev. Lett. **87**, 177006 (2001).
[20] F. Giubileo *et al.*, Phys. Rev. Lett. **87**, 177008 (2001).
[21] H.D. Yang *et al.*, Phys. Rev. Lett. **87**, 167003 (2001).
[22] J.S. Slusky *et al.*, Nature (London) **410**, 343 (2001).
[23] S. Suzuki *et al.*, J. Phys. Soc. Jpn. **70**, 1206 (2001).
[24] O. de la Pena *et al.*, Phys. Rev. B **66**, 012511 (2002).
[25] A. Abragam, *Principles of Nuclear Magnetism* (Clarendon, Oxford, 1961).
[26] Y. Obata, J. Phys. Soc. Jpn. **18**, 1020 (1963); T. Asada and K. Terakura, J. Phys. F: Met. Phys. **12**, 1387 (1982).
[27] H. Kotegawa *et al.*, Phys. Rev. Lett. **87**, 127001 (2001).
[28] J.K. Jung *et al.*, Phys. Rev. B **64**, 012514 (2001).
[29] S.H. Baek *et al.*, Phys. Rev. B **66**, 104510 (2002).
[30] M. Mali *et al.*, Phys. Rev. B **65**, 100518 (2002).
[31] A.P. Gerashenko *et al.*, Phys. Rev. B **65**, 132506 (2002).
[32] H. Kotegawa *et al.*, Phys. Rev. B **66**, 064516 (2002).
[33] J.Y. Xiang *et al.*, Phys. Rev. B **65**, 214536 (2002).
[34] JJ.Q. Li *et al.*, Phys. Rev. B **65**, 132505 (2002).
[35] H.W. Zanbergen *et al.*, Physica C **360**, 221 (2002).
[36] S. Margadonna *et al.*, Phys. Rev. B **66**, 132414 (2002).
[37] E.R. Andrew and D.P. Tunstall, Proc. Phys. Soc. London **78**, 1 (1961).
[38] M.H. Cohen and F. Reif, in *Solid State Physics: Advances in Research and Applications*, edited by F. Seitz, and D. Turnbull (Academic Press, New York, 1957), Vol. 5.
[39] G.C. Carter *et al.*, *Metallic Shifts in NMR*, Progress in Material Science Vol. 20 (Pergamon Press, Oxford, 1977).